# Electrical Characterization of Lead-Free $Na_{0.5}K_{0.5}nbo_3$ Piezoelectric Ceramic / PVA Polymer Composites

**Beena P**

Government First Grade College, Nyamathi – 577223, Davanagere, Karnataka, India

**Abstract**

**Researchers had always focused on materials exhibiting high dielectric properties concerned with storage and dissipation of energy, ferroelectric ceramics which exhibit interesting electrical properties and flexible polymers which will not destroy the behaviour of the ceramics. Sodium potassium niobate ($Na_{0.5}K_{0.5}$ $NbO_3$ or NKN) ceramic was chosen as ceramic and poly vinyl alcohol (PVA) as host polymer matrix in this chapter. NKN was prepared through conventional solid state reaction and PVA/NKN composite films were prepared by solution casting method by changing the blend ratio of PVA and NKN. The prepared samples in the form of films were characterized by powder X-ray diffraction. The SEM studies of composite films reveals that the well dispersion of ceramic crystallites in polymer matrix and the porosity was almost negligible. The frequency dependent dielectric properties of PVA/NKN composites were investigated in the frequency range (100Hz - 5MHz). At room temperature, conductivity and relaxation behaviour of the composites were studied. The contributions of bulk and grain boundaries were confirmed by complex impedance spectroscopy. The complex electric modulus was studied and observed dielectric relaxation behaviour reveals localized hopping of oxygen vacancies.**

**Keywords: Ceramics, Composites, XRD, SEM.**

## Introduction

Materials consisting of more than one kind of substance having different properties are being designed to obtain desirable properties which cannot be obtained from single phase materials. Polymer ceramic composite combines the easy processability and high mechanical strength of polymer and the higher dielectric constant of ceramics. These composites have attracted considerable attention due to potential combination of advanced properties of inorganic and organic components [1]. Piezoelectric materials have become an integral part of today's technology in a multitude of devices such as sensors, actuators, generators, and ultrasonic transducers. etc., [2-4]. But important materials for these applications contain amounts of lead. The lead zirconate titanate (PZT) was used to extract these properties to a highest degree. Now a days, environmental and health concern has led to find lead free materials which could replace PZT [5]. Since lead is highly toxic, there is an increasing interest in developing alternative materials which exhibits piezoelectricity [6]. Among the lead free piezoelectric ceramics, sodium potassium niobate which has a perovskite structure is considered to be one of the most promising candidates [7, 8], that have substituted lead-based piezoelectric materials with relatively large dielectric and ferroelectric properties [9].

In this work the polymer PVA was used as matrix material because of its better aqueous solubility, flexibility, low cost and non-toxicity [10]. NKN was used as filler material. NKN is a ceramic with high curie temperature around 420ºC and a combination of ferroelectric $KNbO_3$ and antiferroelectric $NaNbO_3$ [11]. The enhanced electrical properties of NKN can be obtained near to morphotropic phase boundary where the ratio of K/Na is nearer to 1 [12, 13]. The electrical properties of a polymer/ceramic composite can be controlled by the type of ceramic material used, concentration of the ceramic and interfacial properties of the composites. NKN/PVA composites were fabricated using NKN powder mixed with PVA through solution casting technique. XRD, SEM analysis and dielectric measurements of the composites of different weight % were carried out.

The dielectric constant of the composite can be increased by increasing the ceramic content [14]. In this work, ceramic filler was loaded up to 50% in a polymer which can be easily processed and thereby enhance the dielectric parameters of the composites without damaging the characteristic of pure ceramic material. This study aims at presenting an electrical study of NKN/PVA composites using impedance spectroscopy. The impedance spectroscopy is used as a tool to investigate the effect of interfacial properties in the composites. The complex impedance datas forms a semicircle which is used to understand the grain and grain boundary resistance [15].

## Materials and Method

The powder of NKN ceramics was prepared through conventional solid state reaction route [16]. AR grade sodium nitrate ($NaNO_3$), potassium nitrate (KNO3) and niobium pentoxide ($Nb_2O_5$) precursors were used. Ethylene glycol was chosen as a solvent here because of its high viscosity to form homogenous suspension [17]. $Nb_2O_5$ was added to sodium potassium (Na-K) precursor solution. Then this mixture was heated to 90 ºC and dried on a hot plate to form NKN powder. This NKN powder was calcined at two different temperatures 550 ºC and 850 ºC for 2 hours. The ceramic powders were weighed and transferred into a steel die and pressed uniaxially into green compacts using a load of 200 MPa in hydraulic hands press Vacutech systems VS-201-02.

The chemical reaction is as follows.

The PVA is mixed in 50 ml of hot distilled water. This mixture was continuously stirred at a temperature of 60 ºC for 3 hours and NKN of different weight percentage was added to the above cooled solution and stirred for one hour. This gel type solution is casted on to a glass substrate and allowed to dry at room temperature. The composite films of PVA-NKN of different weight percentage i.e., (100:0), (90:10), (70:30), (50:50) were prepared [18].

The microstructures of films were examined by scanning electron microscopy (SEM) using EVO MA 18 SEM equipped with OXFORD EDS analyser. The x-ray diffraction analysis was performed from 5º to 80º, 2θ values at a step of 4º using Rigaku miniflex 600 diffractometer with a graphite monochromator. For dielectric and ferroelectric studies, silver electrode was deposited on to the film with copper leads. The dielectric constant, tan δ and ac conductivity were measured at room temperature using a PSM1735 LCR meter in the frequency range 100 Hz to 5 MHz. The room temperature P-E hysteresis loops of the composites were analysed using Multiferroic II Ferroelectric tester. The piezoelectric charge coefficient was studied using YE2730A $d_{33}$ Meter, APC International Ltd.

## Results and Discussion

**Powder XRD analysis:** To investigate the phase formation of NKN with increasing calcination temperatures, it was calcined at 550 ºC and 850 ºC for 2 hours in air. The powder calcined at 550 ºC showed the presence of unreacted precursors .This may be due to incomplete reaction of unreacted reactants at lower temperatures. After calcination to 850 ºC, the major Bragg peaks corresponding to expected NKN phase was obtained. All peaks coincided well with those reported earlier suggesting that calcinations temperature at 850 ºC for 2 hours converted the mixed oxides of $KNO_3$, $NaNO_3$ and $Nb_2O_5$ to a single phase which was observed to be a perovskite structure [19]. At 850 ºC, the peaks were shifted to lower side. Hence higher calcination temperature leads to an increase in crystallinity, increase in intensity and decrease in the width of different peaks [20]. The crystallite size of NKN calcined at 850 ºC was calculated to be less than 50 nm.

Similar results are reported earlier [21] and the existence of double structures in figure 1 suggest that NKN exhibits an orthorhombic phase [22]. The cell parameters were calculated from XRD data.

The X-ray diffraction pattern obtained for different weight percentage of PVA / NKN composite shown in figure 2 shows the predominance of NKN phase. In the diffraction pattern of PVA, a major peak of broadness at $2\theta \approx 19.8^{\circ}$ shows the semi-crystalline nature of PVA [23]. The emergent characteristic peaks and their sharpeness increases with filler content. With the increase of NKN ceramic in the NKN/PVA composites, NKN phase starts dominating the properties of the composite.

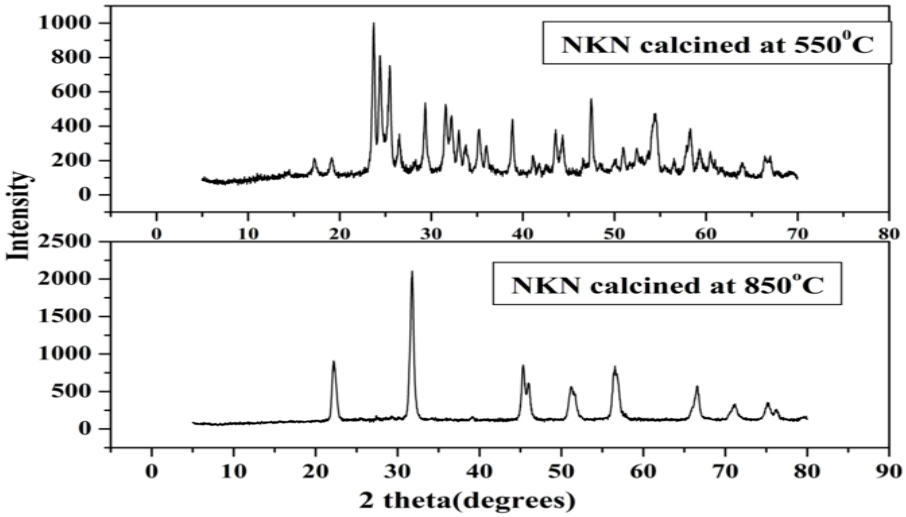


**Figure 1: XRD patterns of NKN ceramic calcined at 550 ºC and 850 ºC**

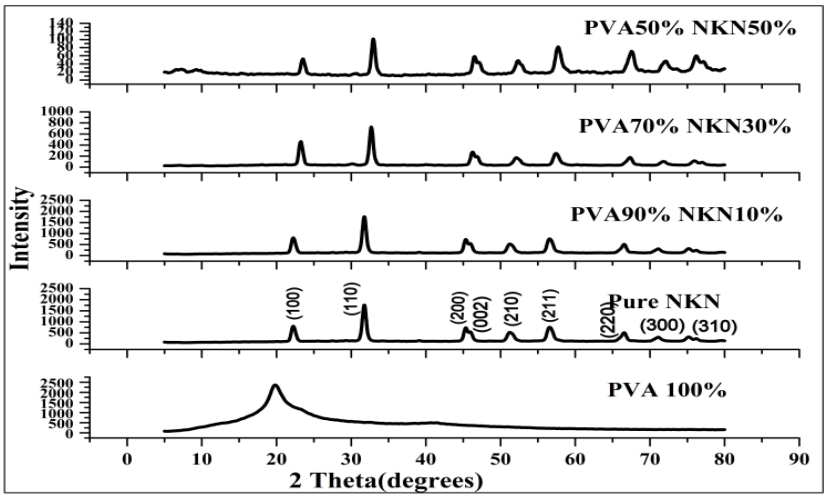


**Figure 2: XRD patterns of PVA-NKN composites calcined at 850 ºC**

As the ceramic inclusion in the polymer increases, shifting of peaks towards the right is observed. This may be due to change in lattice parameters associated with the lattice strain [30].

**SEM analysis**

SEM analysis gives the information about the surface morphology of the sample. The figure 3a shows rod shaped ceramic particles at lower calcinations temperature. These structures were related to relative dissolution rate of reactants. If the dissolution rate of two reactants were different, the reactant with higher rate of dissolution would be dissolved in the solution and would coat onto the reactant with slower dissolution rate. The diffusion between the reactants forms a product layer on surface of the reactant as long as sufficient amount of temperature is provided [24]. The figure 3b shows that, as the calcination temperature is raised the size of rod like structures increases in diameter and decreases in length [25, 26]. The shape and size of the grains and crystallinity depends on the experimental parameters such as reaction temperature, reaction time, solvent type and precursor type [27, 28].

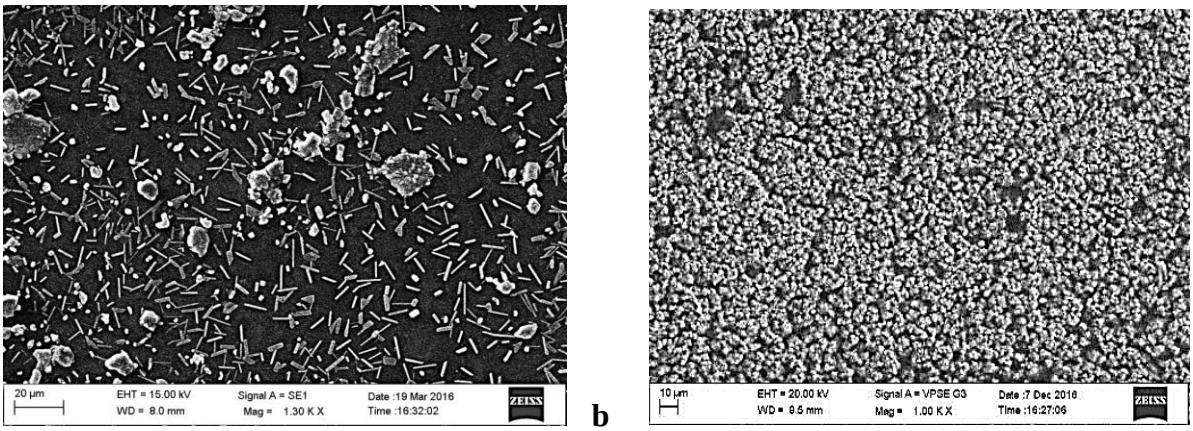


a b

**Figure 3: a) SEM image of NKN calcined at 550 ºC in PVA matrix (70:30)**
**b) SEM image of NKN calcined at 850 ºC in PVA matrix (70:30)**

The agglomeration between the ceramic particles may be due to vanderwaal's forces existing among the particles [29].

**Ac Conductivity Studies:** The cole-cole plots are used to understand the intragrain, grain boundary, electrode effects and relaxation behaviour of the material [31]. At room temperature, the plot of complex permittivity tends to be a straight line with longer slopes for 10% and 30% weight of NKN and this indicates insulating characteristic of the material in figure 4(a). At 50% weight of the ceramic inclusion, a partially formed semi-circular arc was observed at high frequency.

**Table 1: Real and imaginary permittivities and ac conductivity of NKN/PVA composites at 1 MHz)**

| Composition | Real permittivity | Ac conductivity (S/cm) |
|---|---|---|
| PVA 90% NKN 10% | 18 | 0.00048 |
| PVA 70% NKN 30% | 30 | 0.00055 |
| PVA 50% NKN 50% | 17 | 0.00043 |

Experimentally observed dielectric data were fitted into several theoretical models to find the equation required for predicting the effective dielectric constant of the studied composites. Several mixture models had been proposed for predictions of the dielectric constant of two phase heterogeneous systems. The different types of dielectric mixing rules are already discussed in previous chapter. The most commonly used dielectric mixing models are Lichtenecker model [32] and Maxwell's model [33].

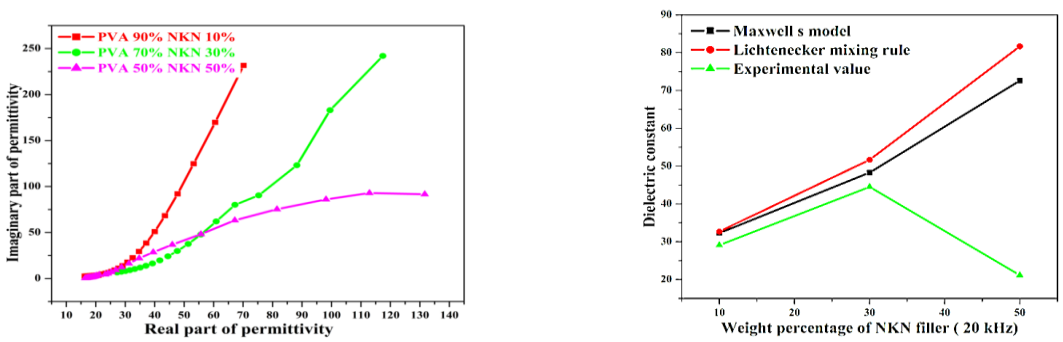


a) b)

**Figure 4: a) Cole-Cole plot of complex permittivity of the composites at room temperature.**
**b) Effective dielectric permittivity from Maxwell and logarithmic mixing rule.**

With the increase in weight percentage of the NKN in the composites, the dielectric constant of the PVA polymer starts differing greatly from the dielectric constant of the NKN particles, the deviation of experimental datas from the theoretical rule begins. The other problem in the prediction of effective dielectric constant of ceramic-polymer composites using theoretical models is the non-availability of dielectric constant of ceramic powders. The dielectric constant of polymer can be obtained by capacitance measurement of the polymer film, but there are no methods to measure the dielectric constant of ceramic powders. Hence, in most literatures the dielectric constant of bulk ceramics were used instead of the dielectric constant of ceramic powders. So the expected dielectric constant values deviates from the measured values at high weight percentage loading [34]. Figure 4b) shows that upto 30 % weight inclusion of NKN, calculated dielectric constant is comparable with that of the above models.

Figure 5(a) shows the variation of ac conductivity of NKN/PVA with frequency. At low frequency, conductivity shows a flat response and is independent of frequencies. But dispersion is observed at higher frequencies which can be explained by the hopping model. Majority charge carriers of perovskites are oxygen vacancies [35, 36]. The conductivity is contributed by the hopping of oxygen vacancies while interacting with the defects of the material. At low frequency, the conductivity is associated with localized ion mobility thereby occupying a neighbouring vacant site. At high frequencies, ion hopping may be unsuccessful and jump back to the previous site and these unsuccessful hops results in dispersion. At room temperature, the observed conductivity of the ceramic composite with 50 % weight NKN concentrations is lower than $5 \times 10^{-7}$ S $m^{-1}$ at 100Hz and this exhibits good dielectric behaviour of the material [37-39].

Applying Jonscher's power law, the slope of log-log curve from figure 5(b) was calculated as 0.432 for 10%, 0.208 for 30% and 0.408 for 50% weight of NKN filler. The observed slope was very low which showed that dc conductivity is negligible.

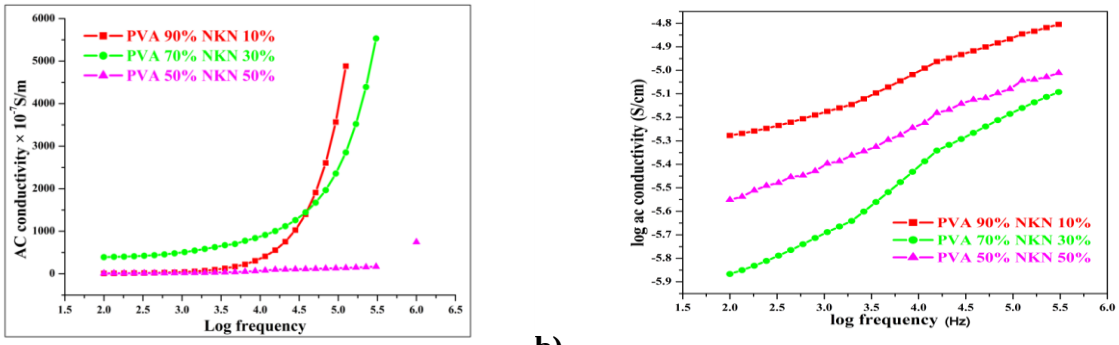


a b)

**Figure 5: a) ac conductivity with frequency of NKN/PVA composites b) log-log curve for Jonscher s power law**

**Complex Impedance and Electric Modulus**

The complex impedance plot is a tool to understand the resistivity of grain and grain boundaries in the material. Figure 6a shows the variation of real part of the impedance (Z') as a function of frequency of the composites at room temperature. From the plot, with rise in frequency, the decrease in the values of $Z^1$ was observed and it showed a flat response above certain frequency. At high frequency, grain and grain boundary resistance decreases and leads to conduction. At lower frequencies, larger polarization in the material leads to higher values of $Z^1$. For pure PVA, $Z^1$ is very low with small variation with frequency. As the ceramic content increases in the composite, there is a drastic increase in $Z^1$ at low frequencies. Above 10 kHz, $Z^1$ is observed to decrease with loading of ceramic filler content and becomes independent of frequency. This conduction may be contributed by the space charge arising from the charges that are trapped at polymer-ceramic interphase [40]. Figure 6(b) shows the variation of imaginary part of complex impedance $Z^{11}$ with frequency at room temperature. The relaxation peaks were observed due to the presence of space charges [41] whose mobility increases at higher frequency indicating conduction process except in case of 50% NKN filler. The peaks were observed at a frequency range 2.6 kHz to 4.7 KHz at room temperature.

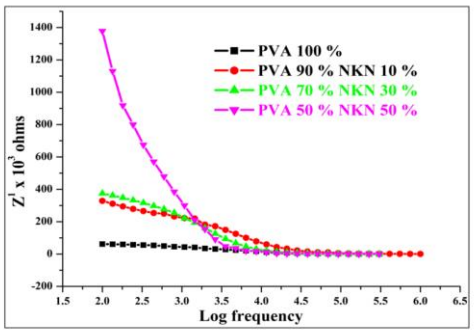


a)

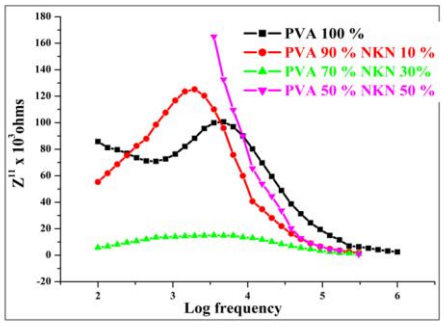


b)

**Figure 6: a) Real part of complex impedance**
**b) Imaginary part of complex impedance with frequency of the NKN/PVA composite**

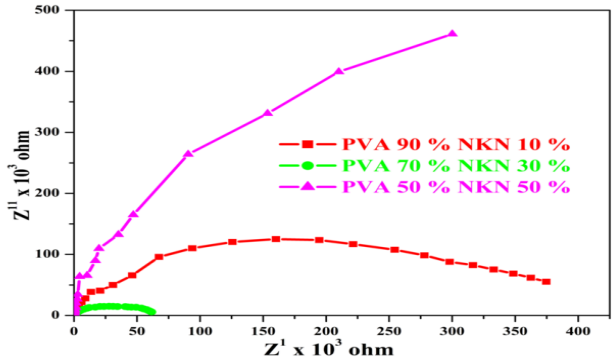


**Figure 7: Cole-cole plot of complex impedance for NKN/PVA composites**

The complex impedance spectra ($Z^{11}$ v/s $Z^{1}$) at room temperature is shown in figure 7. The impedance spectrum is always explained by the semicircles. The semicircle formed at low frequency corresponds to the grain boundary effect and semicircle at high frequency to grain resistance [42]. In the composite of 30% weight of NKN, the curve bends into semicircle which indicates a contribution of intra grains alone thereby indicating a single relaxation phenomenon. The other two composites showed a tendency to bend to form a semi-circular arc and these composites may have more than one relaxation and broad peaks indicates the distribution of relaxation time and these relaxation processes may be a mixture of both ionic motion and polymer segmental motion[43]. These relaxations can be due to the decay of polarization in oxygen-defect dipoles.

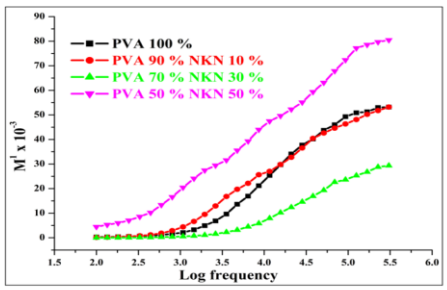


a)

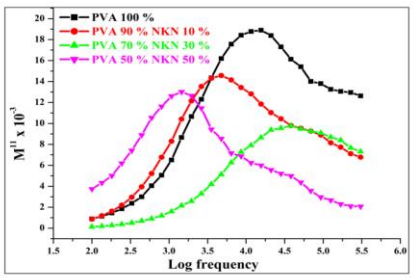


b)

**Figure 8: a) Real part of complex modulus**
**b) Imaginary part of complex modulus vs frequency of NKN/PVA composites**

The complex modulus analysis is a tool to understand the electrical properties of the material such as ion hopping rate, conductivity and relaxation time. The figure 8(a) shows the variation of real part of complex electric modulus $M^1$ with frequency of NKN/PVA composites at room temperature. From the graph, it was observed that the value of $M^1$ in all the composites was almost zero at lower frequencies and is associated with electrode/ionic polarization [44]. But $M^1$ continuously increases with increase of frequency and finally tends to saturates at

higher frequencies. The saturation behaviour can be a resultant of conduction phenomenon due to short-range mobility of charge carriers [45]. Figure 8(b) shows the plot of imaginary part of complex modulus $M^{11}$versus frequency. The peaks were observed in all composites. The region on left side of the peak is associated with conduction process, while region on the right side of the peak associated with the relaxation process where the ion can make localized motion within the neighbouring sites [46]. The conduction in material takes place through ion migration between vacant sites of the polymer along with the segmental relaxation of the polymer. The lack of symmetry in broadening of peak shows the spread of relaxation time [47].

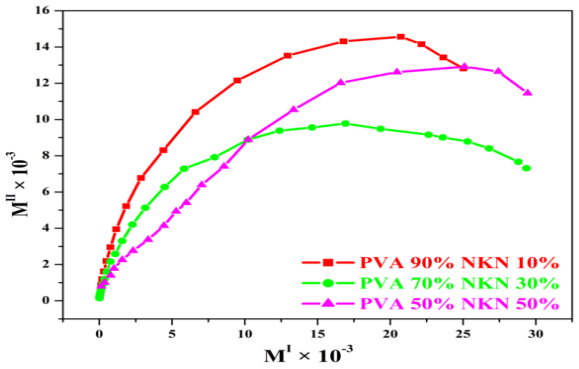


**Figure 9: Electric modulus cole cole plot of NKN-PVA composites**

From figure 9, the cole cole plot shows incomplete semicircles and intercept of these semicircles indicates the total capacitance contributed by the grain and the intercept of second semicircle indicates the total capacitance contributed by the grain boundary which is absent in this plot.

**Dc Conductivity Studies:** The dc conductivity study helps to illustrate not only the effects of grain orientation, but also the nature of charge carrier. The estimated activation energies of the material system may correspond to the motion of oxygen vacancies in the octahedron of the perovskite structure. The slope of Arrhenius plot log ($\sigma_{dc}$) versus $10^3$/T plots in figure.10 yielded the values of ($-E_a/k_B$) and by multiplying by Boltzmann constant $k_B$= 1.381 × $10^{-23}$ J/K, activation energy for dc conductivity can be calculated. At higher temperatures dc conductivity is more dominant which indicates semiconducting behaviour of the material system.
The conductivity increases with weight percentage of the composite. Activation energy of PVA/NKN composite on an average is 0.243eV for 10%, 0.234eV for 30% and 0.209eV for 50% weight of ceramic inclusion. These activation energy shows that the main contribution to polarization is due to electronic conduction process via oxygen vacancy migration [48, 49].
Studies shows that perovskites such as NKN contains intrinsic defects, which are vacancies on the A (Na and K) sites and the O sites. Increase in the A-site vacancies, increases the resistivity or decreases the conductivity of the perovskites. The free electrons present in the material are captured by the electron holes created at the A-site vacancies. So only few electrons are available to freely conduct, thereby exhibiting insulative properties.

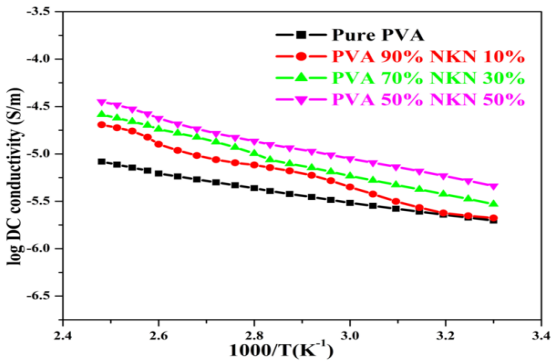


**Figure 10: log dc conductivity vs $10^3$/T of PVA/NKN composites**

**Ferroelectric and piezoelectric studies**

When comparing the hysteresis loop of NKN composites (Figure 4.16), the 10% NKN composite shows poor saturation. This is due to low dielectric, non-piezoelectric polymer layer between the NKN fillers, shielding the ceramic particles from the applied electric field thereby lowering the polarization of the NKN. A further increase in the applied driving voltage led to electric arcing between the electrodes making it impossible to apply electric field more than 4 kV/cm. But 50% NKN composite exhibited a better saturation loop comparitively. When the field was increased, the composite breaks down and a fully complete saturated loop could not be acquired [50]. A fully saturated loop shows that the domains are fully switched and aligned with the direction of the applied field in both directions

The hysteresis behaviour of NKN composites were investigated. P-E hysteresis loops shows better saturation on increasing the weight of NKN in the the composite matrix. The measured parameters are listed in table 2. A comparison of P-E loops in figure 11 (b) reveals that both remnant polarization (Pr) and saturation polarization ($P_{sat}$) increase with increase in applied electric field**.**

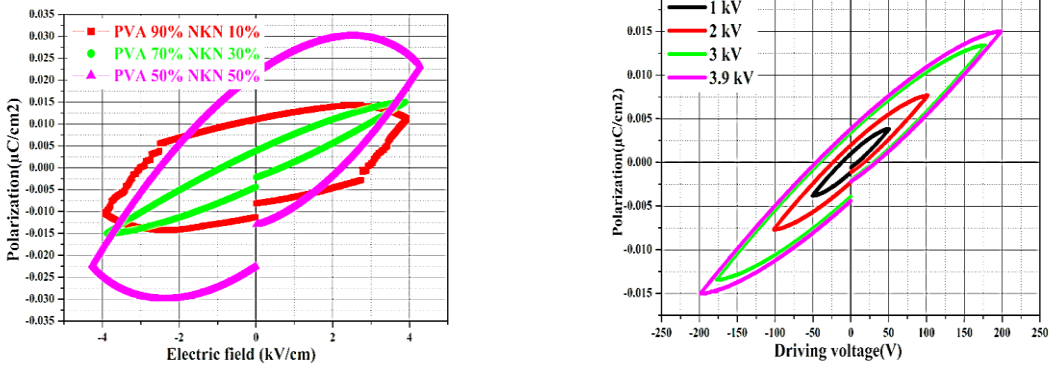


**a)** **b)**

**Figure 11: a) P-E curve of NKN/PVA composites**
**b) P E loops of 30% NKN at different fields**

**Table 2: Ferroelectric parameters of NKN composites**

| Composites | $P_{sat}$ (μC/cm2) | $P_r$ (μC/cm2) | $E_c$ (kV) | Loop area (μC/cm2·volts) |
|---|---|---|---|---|
| 10% NKN | $1.12\times10^{-2}$ | $1.11\times10^{-2}$ | 2.85 | 6.59 |
| 30% NKN | $1.50\times10^{-2}$ | $3.85\times10^{-3}$ | 0.55 | 2.06 |
| 50% NKN | $2.34\times10^{-2}$ | $2.16\times10^{-2}$ | 2.16 | 8.43 |

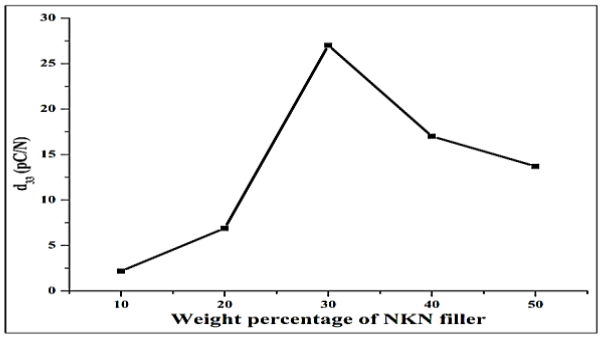


**Figure 12: Piezoelectric charge coefficient of NKN composites**

In this study, the composite samples were poled at room temperature. When a force of 0.25N was applied on an area 1cm$^2$ of a poled sample by the upper and lower probes, piezoelectric charges were produced due to the piezoelectric effect on the contact area. Hence, piezoelectric charge coefficient ($d_{33}$) was measured by measuring the charge developed on the surface of the sample. Average $d_{33}$ values were calculated after taking measurements from various areas across a ceramic composite sample.

The piezoelectric constant ($d_{33}$) of the NKN-PVA composite samples are shown in figure 12. Maximum $d_{33}$ value ~ 27.5 pC/N is obtained in case of 30% NKN-70% PVA composite. The piezoelectric constant is strongly dependent on the domain orientation during poling. In this case, during poling process the domain orientation appears to be more due to better connectivity [51]. The piezoelectric studies of composites shows piezoelectric charge coefficient $d_{33}$ of the composites vary from 2 pC/N at 10%, 27.5 pC/N at 30% inclusion of NKN and then decreased to 13 pC/N at 50% inclusion.

## Conclusions

The NKN was synthesized through solid state reaction route. The optimized calcination temperature of NKN ceramics was 850˚C for 2 h. PVA/NKN ceramic-polymer composite thick films with 10, 30 & 50 weight percentage) were synthesized by solvent cast method. The XRD patterns of the composite specimens showed the dominated phase of ceramic. Higher calcination temperature of the ceramic led to an increase in crystallinity, increase in intensity of different peaks and decrease in their widths. The morphological studies confirmed the 0-3 connectivity and homogeneity of the ceramic powder distribution with the increase of ceramic particles content in the composites. The AC conductivity is explained by the hopping model where localized ion hopping is observed at low frequency and unsuccessful hops of ions results in dispersion at high frequencies. The cole cole plots of complex impedance showed only one semicircle at high frequency which corresponds to intragrain effect. The electric modulus peak area explains the transformation of long range mobility of ion/charge carriers to short range mobility. The obtained results suggests the suitability of PVA/NKN composite with 30% ceramic for embedded capacitor and piezoelectric applications

## References


1. Peter Barber and Shiva Balasubramanian, et al. *Materials*, 2, (2009) 1697.
2. Canhan Sen, Berk Alkan, Ipek Akin, et al. *J. Ceram. Soc.* Japan, 119(5), (2011) 355.
3. Kiyoshi Kanie, Yoshiki Numamoto, Shintaro Tsukamoto, et al. *Mater. Transac*, 52(11), (2011) 2119-2125.
4. Wen Chen, Jinyan Zhao, Lingyan Wang, et al. *AIP Advances*, 5, (2015) 077190.
5. Gao F, Liu L, Xu B. *J. Euro. Cera. Soc.* 31, (2011) 2987-2996.
6. Sebastian Wiegand, Stefan Flege, Olaf Baake et al. *J. Mater. Sci. Technol*., 28(6), (2012) 500(505).
7. Jin Qiu Zhao, Yan-Gai Liu, Ming-Hao Fang, et al. *J Electro. Ceram*, 2014; 32, 255.
8. Beena P, Jayanna H S, Desai N B, *J. Poly. Comp*., 6(1), (2018)1-8.
9. Bhatt S C and Manish Uniyal. Inter. *J. Mater and Chem*., 2(2), (2012) 47.
10. Shinichiro Kawada, Hiroyuki Hayashi, Hideki Ishii, et al. *Materials* 8, (2015), 7423–7438.
11. Ramesh Babu, Vijaya Kumar K. Inter. *J. Chem Tech Research*, 7(01), (2015) 171-180.
12. Shirane G, Newnham R and Peinsky R. *Phys. Rev*., 96, (1954) 581 -588.
13. Canhan Sen, Berk Alkan, Ipek Akin, et al. *J Ceram Soc Japan* 119(5), (2011) 355–361.
14. Zhang B P, Li J F, Wang K, et al. *J. Am. Ceram. Soc*. 89, (2006) 1605-1609.
15. Jung-Rag Yoon, Jeong-Woo Han, Kyung-Min Lee. Trans. *Electr. And electron. Mater*. 10(4), (2009) 116-120.
16. Ebru Mensur Alkoy, Ayse Berksoy-Yavuz. *IEEE Trans. Ultrason. Ferroelectr. Freq. Contr*. 59(10), (2012) 2121-2128.
17. Barbara Malic, Jurij Koruza, Jitka Hrescak, et al. *Materials*. 8, (2015) 8117–8146.
18. Huidong Li. *Sodium Potassium Niobate-based Lead-free Piezoelectric Ceramics: Bulk and Freestanding Thick Films*, PhD Thesis, Philadelphia, US, Drexel University, 2008.
19. Beena P, Jayanna H S and Desai N B. *J. Polymer and Composites*. 6(1), (2018) 1-8
20. Pornsuda Bomlai, Winai Saengchote, Supasarote Muensit, et al. *J. Sci. Technol*., 29(2), (2007) 441.
21. Nobre M A L and Lanfredi S. *Catalysis Today*. 78, (2003) 529.
22. Mahesh P and Pamu D. *IOP Conf. Series: Materials Science and Engineering*, 73, (2015) 012141.
23. Darja Jenko, Andreja Bencan, Barbara Malic, et al. *Microsc. Microanal*. 11, (2005) 572–580.
24. Ahmed K, Kanwal F, Ramay S M, et al. Digest. J. *Nanomater. Biostructures*, 12(3), (2017) 775.

25. Li Ting Tseng, Xi Luo, Thiam Teck Tan, et al. *Nanoscale.Res*. Lett. 9(1), (2014) 673
26. Asha Dahiya and Thakur O P. Inter. *J. Engg and Inno. Technology (IJEIT*). 3(8), (2014) 176.
27. Xinyu Zhang, Jiaquan Qin, Yanan xue, et al. *Scientific report 4*, (2014) Article no. 4596.
28. Yongming Hu, Haoshuang GU and Zhao Wang. *Nanowires-Fundamental Research* (Intech Open 564, 2011).
29. Cheng Yan Xu, Liang Zhen, Rusen Yang , et al . *J. Am. Chem. Soc*. 129, (2007) 15444-15445.
30. Thomas P, Satapathy S, Varma K B R, et al. *eXPRESS Polymer Letters*, 10, (2010) 632–643.
31. Rancourt D G, Meunier R F. *American Mineralogist 93*, (2008) pp 1412–1417.
32. Ansu Kumar Roy, Amrita Singh, Karishma Kumari, et al. *IOSR Journal of Applied Physics* 3(5), (2013) 47-58.
33. Goncharenko A V, Lozovski V Z and Venger E F. *Optics Communications*. 174 (2000) 19.
34. Thomas P, Varughese K T, Dwarakanath K, et al, *Composites Science and Technology*. 70 (2010) 539.
35. Cho S, Lee S, Hyun J, et al. *J. Mater. Science: Mater.in Electronics 16* (2005) 77– 84.
36. Dasari M P, Sambasiva Rao K, Murali Krishna P, et al. *ACTA PHYSICA POLONICA A*, 119(3), (2011) 387-394.
37. Pelaiz-Barranco A. *J. App. Phy.102*, (2007) 114102.
38. Elliot S R. *Adv. Phys 36*, (1987) 135–217.
39. Funke K. *Progress in Solid State Chemistry* 22(2), (1993) 111–195.
40. Forbess M J, Seraji S, Wu Y, et al. *Appl. Phys. Lett* 76, (2000) 2934–2936.
41. Amrita Singh, Kumar Amarnath, Kamal Prasad, et al. *IOSR Journal of Applied Physics* 7(2), (2015) 17-26.
42. Ganguly P, Jha A K, Deori K L, *Solid State Commun*. 146, (2008) 472–477.
43. Shujahuddeen B. Aziz. *Bull. Mater. Sci*. 38(6), (2015) 1597–1602.
44. Chian Heng Lee, Jumiah Hassan, Mansor Hashim, et al. *J. Adv. Dielect* 4(4), (2014) 1450034 (8 pages).
45. Pritam Kumar, Ajay Kumar Sharma, Bhrigunandan Prasad Singh, et al. *Materials Sciences and Applications* 3, (2012), pp369-376.
46. Jacob R, Nair H G, Isac J. *Proc. Appl. Ceram* 9(2), (2015) 73–79.
47. Praveen Khatri, Banarji Behera, Srinivas V, et al, *Research Letters in Materials Science* 2008, (2008) Article ID 746256, 5 pages.
48. Woan, G., *The Cambridge Handbook of Physics Formulas*. (Vol. 2003 Edition: Cambridge University Press, New York, USA).
49. Matsudo, H., K.-I. Kakimoto, and I. Kagomiya, *Key Engineering Materials.* 421-422 (2010) 9-12.
50. Zhang S, et al., *Journal of Applied Physics*, 100, (2006) p. 104108-1-6.
51. Le D T, Do N B, Kim D U, et al. *Ceram. Int*. 38, (2012) S259.